

STRENGTH OF COMPOSITE BEAMS WITH WEB OPENINGS

by

DAVID MARTIN TODD

B. S., Kansas State University, 1977

---

A MASTER'S THESIS

Submitted in partial fulfillment of the  
requirements for the degree


MASTER OF SCIENCE

Department of Civil Engineering

KANSAS STATE UNIVERSITY  
Manhattan, Kansas

1979

Approved:

  
Major Professor

Spre Coll.  
LD  
2668  
T4  
1779  
T62  
C.2

TABLE OF CONTENTS

	Page
INTRODUCTION. . . . .	1
Problem Statement and Scope. . . . .	1
Review of Previous Ultimate Strength Analyses. . . . .	1
ULTIMATE STRENGTH ANALYSIS. . . . .	5
Assumptions. . . . .	5
Outline of Solution. . . . .	5
Development of Basic Equations . . . . .	6
Reference Values. . . . .	6
Low Shear Solution. . . . .	8
High Shear Solution . . . . .	13
Calculation of Interaction Diagrams. . . . .	15
TYPICAL RESULTS AND DISCUSSION. . . . .	19
Interaction Diagrams . . . . .	19
Effects of Varying Key Parameters. . . . .	21
Comparison with Experimental Results . . . . .	22
CONCLUSIONS . . . . .	24
RECOMMENDATIONS FOR FURTHER RESEARCH. . . . .	25
ACKNOWLEDGMENTS . . . . .	26
APPENDICES. . . . .	27
I. References . . . . .	27
II. Notation . . . . .	28
III. Computer Program . . . . .	31
FIGURES . . . . .	39

## INTRODUCTION

### Problem Statement and Scope

The objective of this thesis is to present an ultimate strength analysis of composite beams with web openings. A composite beam is defined as a steel W shape acting together with a concrete slab to resist transverse loads. An opening located in the web of the steel section is usually introduced to permit the passage of utility ducts and piping. Figures 1 and 2 show elevation and cross section views of a composite beam with a web opening.

The analysis is limited in scope by the physical characteristics of the beam, and the type of failure assumed at the opening. The slab thickness is limited to the range of values normally encountered in practice, and the slab width is taken to be the effective width, which is determined in the usual manner (11). A sufficient number of shear connectors are assumed to be present so that full composite action is attained. The opening is limited to a rectangular shape, which can be located anywhere on the span, and can be concentric (mid-depth of opening coincides with mid-depth of steel shape) or eccentric. Only unreinforced openings are considered. Failure is limited to yielding only, i.e., buckling and instability failures are not considered.

### Review of Previous Ultimate Strength Analyses

In the past decade a number of investigators have developed ultimate strength analyses of non-composite beams with rectangular web openings. All of these analyses lead to the development of an interaction diagram which shows the relationship between moment and shear acting at an opening at failure. Several basic assumptions are common to these

analyses. A failure mechanism is assumed to form with plastic hinges located at the sections above and below each edge of the opening. Failure due to instability is not considered. Equilibrium conditions are satisfied. Yielding occurs in the flanges due to tension or compression, and yielding in the web due to combined shear and normal stresses follows von Mises yield criterion (10). The presence of shear causes secondary moments in the top and bottom sections. None of the analyses take into consideration the beneficial effect of strain hardening.

The first analysis, which was concerned with concentric openings with no reinforcement, was developed by Bower (1). The possibility of the web and flanges having different yield stresses was provided for in this analysis. The shear force was applied only to that portion of the web which was also assigned the secondary moment. Later, in dealing with the same case, Redwood chose to have the same yield stress throughout the section, and also assigned the shear force uniformly along the total depth of the remaining web (7). Redwood's revisions were incorporated into subsequent analyses of concentric reinforced openings by Congdon and Redwood (2), eccentric unreinforced openings by both Frost (4) and Richard (8), and the most general case of eccentric reinforced openings by Wang (12).

New insight for the analysis of beams with web openings was presented in a report by McCormick (6). By the use of two new concepts, McCormick developed a much simpler analysis than any of those previously presented. One of these concepts is to assign a moment due to eccentricity,  $M_e$ , in the larger tee section to represent the stresses in that section. As in previous analyses, the shear force was assigned to the full web stub



length, but in applying von Mises criterion the web thickness was reduced according to the value of shear present, so that the effect of the shear stress can be ignored throughout the remainder of the calculations. Because of these new concepts--introduction of  $M_e$  and reduction of the web thickness for shear--axial forces and moments, instead of stress blocks, were used in a statical method for a lower bound approach which leads to a simpler analysis.

A comparison between Redwood's and McCormick's analyses was made by Scritchfield, who concluded that "McCormick's method of analysis was found to be better suited for extension to the eccentric case" (9). Scritchfield applied McCormick's method to the case of eccentric unreinforced web openings by the use of a computer program, which when compared with earlier programs using Redwood's method, gave the same results. It was also proved that the points of contraflexure are at the center of the opening.

The only material reviewed pertaining to ultimate strength analysis of composite beams with web openings was that found in McCormick's report (6). In the report, McCormick performs an analysis of a specific composite beam with known dimensions and material properties, having two circular web openings with varying types of reinforcement. The assignment of internal forces is carried out in a manner similar to that used for non-composite beams. The concrete slab is assumed to carry no shear. An equivalent rectangular opening having a depth of  $0.9D$  and a width of  $0.45D$ , where  $D$  is the diameter of the circular opening, is assumed for the failure mode consisting of a four hinge mechanism at one opening. McCormick also assumes a constant distance between the axial forces in the top and bottom tees instead of determining this distance from beam properties for each value of total shear force.

The analysis presented in this thesis has many assumptions in common with McCormick's analysis, but is developed for general beam geometry and material properties, and for a single rectangular opening of any practical depth, width, and position.

## ULTIMATE STRENGTH ANALYSIS

### Assumptions

The ultimate strength analysis is based on the following assumptions:

1. The compressive strength of the concrete in bending is assumed to be  $0.85 f'_c$  and the Whitney stress block is used.
2. The tensile strength of the concrete is neglected; therefore yielding in the concrete is by compression only.
3. Yielding in the steel flanges is by compression or tension only.
4. Shear, which causes secondary bending in the sections above and below the opening, is carried in the web only, and is uniformly distributed.
5. Yielding in the web of the steel section due to combined shear and normal stresses follows von Mises yield criterion.
6. Equilibrium is satisfied.
7. Points of contraflexure occur at the midpoints of the sections above and below the opening.
8. Failure occurs by the formation of a mechanism with hinges at sections above and below the edges of the opening. (Fig. 3).
9. The possibility of failure due to instability and the beneficial effects of strain hardening are not considered.

### Outline of Solution

The solution is divided into two parts, designated Case I and Case II. Case I is called the low shear case, during which all of the total shear force,  $V$ , assigned to the beam is carried by the top tee, i.e., the shear in the top tee,  $V_T$ , equals the total shear  $V$ . Because no shear force is assigned to the bottom tee in Case I, the capacity of the bottom tee is used solely for the axial force  $P_B$ , which, when combined with an equal force in the slab, gives the primary moment,  $P_B d_c$ .

A special situation to consider at the outset of Case I is that of pure bending, i.e.  $V = 0$ , (Fig. 4a). The total capacity of the top tee is assigned to the axial force  $P_T$ , which, when combined with an equal

force in the slab, results in the moment due to eccentricity,  $M_e = P_T d_e$ . The moment capacity at the centerline of the opening is the sum of the primary moment,  $P_B d_c$ , and  $M_e$ .

When the shear force in Case I is non-zero, the web thickness,  $t_w$ , of the top tee is reduced to  $w_T$  according to von Mises yield criterion, so that all the fibers in the reduced steel section will be at the yield stress. A secondary moment due to shear,  $M_{VT} = V_T a$  is induced in the top tee (Fig. 4b). This causes a reduction in  $P_T$  and likewise in  $M_e$ . The total moment capacity at the centerline of the opening is still the sum of the primary moment,  $P_B d_c$ , and  $M_e$ . The upper limit of Case I is reached when the total top tee is yielded due to  $V_T$  and  $M_{VT}$ , so that  $M_e$  is equal to zero.

Case II (Fig. 4c) is called the high shear case during which part of the total shear goes to the top tee and the rest goes to the bottom tee. The amount of the total shear assigned to the top tee is governed by the capacity of the top tee section for  $V_T$  and  $M_{VT} = V_T a$ . The amount of shear remaining when this capacity is reached is the shear assigned to the bottom tee,  $V_B$ . With shear present, the web thickness of the bottom tee is reduced to  $w_B$ , and a secondary moment due to shear,  $M_{VB} = V_B a$ , is induced. The axial force  $P_B$  is assigned to that portion of the bottom tee not used for  $V_B$  or  $M_{VB}$ . The force  $P_B$ , along with an equal force in the concrete slab, gives the primary moment, which is the total moment capacity at the centerline of the opening, because  $M_e$  is zero throughout Case II.

#### Development of Basic Equations

Reference Values. At the outset, a number of reference values are defined. The length of the web stubs above and below the opening are (Fig. 2)

$$s_T = \frac{1}{2} d - e - h - t \quad (1)$$

$$s_B = \frac{1}{2} d + e - h - t \quad (2)$$

The shear capacities of the top and bottom web stubs by definition are

$$V_{yT} = \frac{s_T t_w F_y}{\sqrt{3}} \quad (3)$$

$$V_{yB} = \frac{s_B t_w F_y}{\sqrt{3}} \quad (4)$$

From Fig. 5a, the shear capacity of the web without the opening (the gross web area) is

$$V_P = \frac{(d-2t)t_w F_y}{\sqrt{3}} \quad (5)$$

The total plastic moment of the gross composite section,  $M_{Pc}$ , is the final reference value required. Two expressions for  $M_{Pc}$  are possible depending on the location of the plastic neutral axis,  $NA_P$  of the gross composite section. To determine where this neutral axis is, a comparison is made between the total axial force capacity of the concrete slab

$$P_{yc} = b_c c F_c \quad (6)$$

and the total axial force capacity of the gross steel section

$$P_{ys} = (t_w(d-2t) + 2bt)F_y \quad (7)$$

If  $P_{yc}$  is greater than  $P_{ys}$ , then the  $NA_P$  is in the concrete slab as shown in Fig. 5a. The thickness of concrete used to give a force in the concrete slab equal to that of the steel section is given by

$$c_{Ps} = \frac{P_{ys}}{b_c F_c} \quad (8)$$

This is the thickness of the concrete above the  $NA_P$ ; the concrete below the  $NA_P$  is disregarded or "thrown away" because it is in tension. The

value of the total plastic moment is found by summing the moments about the  $NA_p$  resulting in

$$M_{Pc} = (\frac{1}{2}bc c_{PS}^2)F_c + (\frac{1}{2}d + c - c_{PS})P_{ys} \quad (9)$$

If  $P_{yc}$  is less than  $P_{ys}$ , the  $NA_p$  is in the top steel flange as in Fig. 5b. To find its location, a thickness  $t_t$  is assigned to the portion of the flange which is in tension below the  $NA_p$ . By setting the forces above and below the  $NA_p$  equal to each other, the value of  $t_t$  is

$$t_t = \frac{b_c c F_c - t_w (d-2t) F_y}{2b F_y} \quad (10)$$

Now by summing moments about the  $NA_p$ , the total plastic moment is

$$M_{Pc} = b_c c (\frac{1}{2}c + t - t_t) F_c + [t_w (d-2t) (\frac{1}{2}d - t + t_t) + \frac{1}{2}b(t-t_t)^2 + \frac{1}{2}bt_t^2 + bt(d - \frac{3t}{2} + t_t)] F_y \quad (11)$$

Low Shear Solution. The following discussion of the analysis is divided into two major parts: Case I being the low shear case and Case II being the high shear case. In Case I, the total shear force is applied to the top tee, i.e.  $V_T = V$ . In assigning this shear force to the web, a portion of the web thickness is removed due to yielding in shear and with the use of von Mises yield criterion, the remaining web thickness used to carry normal stresses is

$$w_T = t_w \sqrt{1 - 3 \left( \frac{V_T}{s_T t_w F_y} \right)^2} \quad (12)$$

When  $V_T$  is equal to zero the special case of pure bending occurs. In this case, the secondary moment due to shear,  $M_{VT}$ , is equal to zero and  $w_T$  equals  $t_w$ .

Because no shear is applied to the bottom steel tee, it provides a constant axial tensile force,  $P_B$ , throughout the low shear case (Fig. 6)

$$P_B = (t_w s_B + bt) F_y \quad (13)$$

Force  $P_B$  has a corresponding compressive force in the concrete slab. The thickness of the concrete slab required for  $P_B$  is assigned starting from the top of the slab and is determined by

$$c_{PB} = \frac{P_B}{b \cdot F_c} \quad (14)$$

The forces in the bottom tee and concrete slab combine to give the primary moment. To find this moment, the distance between the centroids of the two forces must be found. From Fig. 6, the distance from the top edge of the opening to the line of action of the force in the concrete slab is

$$y_c = s_T + t + c - \frac{1}{2}c_{PB} \quad (15)$$

while the distance from the bottom edge of the opening to the line of action of the force in the bottom tee is

$$y_B = \frac{\frac{1}{2}t_w s_B^2 + bt(s_B + \frac{1}{2}t)}{t_w s_B + bt} \quad (16)$$

The lever arm of these forces is

$$d_c = y_c + 2h + y_B \quad (17)$$

thus the primary moment is defined as the product,  $P_B d_c$ .

There are two cases to consider in the low shear analysis of the top steel tee - concrete slab section shown in Fig. 7 after the portion of the slab due to the primary moment is removed. These are Case IA in which all the remaining slab in Fig. 7 is used and Case IB in which only part of the slab is used. The location of the  $NA_p$  in the flange or the slab of the section in Fig. 7 determines at the outset which case applies. To determine this location, the axial force capacities of the slab with thickness

$$c_r = c - c_{PB} \quad (18)$$

and the steel tee are required. They are respectively, (Fig. 7)

$$P_{ycr} = b_c c_r F_c \quad (19)$$

and

$$P_{yT} = (s_T w_T + bt) F_y \quad (20)$$

If  $P_{ycr}$  is less than  $P_{yT}$ , then the  $NA_p$  is in the flange. Referring to Fig. 8, the distance to the  $NA_p$  in the flange is found by setting the forces above and below equal to each other resulting in

$$y = s_T + \frac{1}{2}t - \frac{s_T w_T}{2b} + \frac{b_c c_r F_c}{2b F_y} \quad (21)$$

Now the total moment capacity of this section by summing the moments about the  $NA_p$  is

$$\begin{aligned} M_{cap} = & b_c c_r (s_T + t - y + \frac{1}{2}c_r) F_c + [s_T w_T (y - \frac{1}{2}s_T) \\ & + \frac{1}{2}b (y - s_T)^2 + \frac{1}{2}b (s_T + t - y)^2] F_y \end{aligned} \quad (22)$$

When a non-zero shear is imposed, a certain portion of the top steel tee is assigned a moment due to shear

$$M_{VT} = V_T a \quad (23)$$

This shear moment is assigned to the extreme top and bottom edges of the steel tee moving inward and is restricted by the location of the  $NA_p$  shown in Fig. 9. The portion of the flange above the  $NA_p$  is

$$t_v = s_T + t - y \quad (24)$$

and a depth of web

$$s_v = \frac{b t_v}{w_T} \quad (25)$$

is found such that the area of the flange above the  $NA_p$  is equal to the area of the web corresponding to the depth  $s_v$ . If  $s_v$  is less than  $s_T$  as



shown in Fig. 9a, then the distance between the centroids of the two forces is  $s_T + t - \frac{1}{2}t_V - \frac{1}{2}s_V$ , and the maximum  $M_{VT}$  allowed is the force times its lever arm

$$M_{Vmax} = bt_V(s_T + t - \frac{1}{2}t_V - \frac{1}{2}s_V)F_y \quad (26)$$

When  $s_V$  is greater than  $s_T$  (Fig. 9b), the bottom portion of  $M_{VT}$  goes into the flange a thickness

$$t_{Vw} = \frac{-s_T w_T + bt_V}{b} \quad (27)$$

Summing moments about the  $NA_p$  gives

$$M_{Vmax} = [s_T w_T (y - \frac{1}{2}s_T) + \frac{1}{2}bt_V^2 + bt_{Vw}(t - \frac{1}{2}t_{Vw} - t_V)]F_y \quad (28)$$

In both cases ( $s_V$  greater than or less than  $s_T$ ), if  $M_{VT}$  is less than  $M_{Vmax}$ , then the moment due to eccentricity is

$$M_e = M_{cap} - M_{VT} \quad (29)$$

and the total moment capacity of the beam with the web opening is

$$M = P_B d_c + M_e \quad (30)$$

When  $M_{VT}$  is greater than  $M_{Vmax}$ , part of the slab is "thrown away" and Case IB is encountered.

Case IB with the  $NA_p$  in the slab also occurs when  $P_{ycr}$  is greater than  $P_{yT}$  (Fig. 7). This second major breakdown of the low shear case has two further divisions - if  $s_V$  (as described previously) is less than or greater than  $s_T$ .

When  $s_V$  is less than  $s_T$  as in Fig. 10a, knowing that the areas in the web and flange must be equal, the thickness of the flange used for  $M_{VT}$  is

$$t_V = \frac{s_V w_T}{b} \quad (31)$$

Using the force and lever arm,  $M_{VT}$  becomes

$$M_{VT} = s_V w_T (s_T + t - \frac{1}{2} t_V - \frac{1}{2} s_V) F_y \quad (32)$$

but is also equal to  $V_T a$ . Setting these two equations equal and substituting for  $t_V$  gives

$$\left(\frac{1}{2} + \frac{w_T}{2b}\right) s_V^2 - (s_T + t) s_V + \frac{V_T a}{w_T F_y} = 0 \quad (33)$$

This quadratic equation can be solved for  $s_V$ , after which  $t_V$  can be determined from Eq. 31. Now the remaining portions of the web

$$s_P = s_T - s_V \quad (34)$$

and the flange

$$t_P = t - t_V \quad (35)$$

are used to find the axial tensile force component of  $M_e$  which is

$$P_T = (s_P w_T + b t_P) F_y \quad (36)$$

An equal force is assigned in the slab starting down at the point where  $c_{PB}$  stops until the thickness as given by

$$c_{PT} = \frac{P_T}{b_c F_c} \quad (37)$$

is reached. Summing the moments of these two forces about the  $NA_p$  (which is at the bottom of the slab being used) gives

$$M_e = \frac{1}{2} b_c c_{PT}^2 F_c + [s_P w_T (c_r - c_{PT} + t + \frac{1}{2} s_P) + b t_P (c_r - c_{PT} + t_V + \frac{1}{2} t_P)] F_y \quad (38)$$

When  $s_V$  is greater than  $s_T$ , the bottom portion of  $M_{VT}$  goes into the bottom of the flange as in Fig. 10b. The thickness of flange above line XX on the top tee steel section now becomes by setting the forces above and below line XX equal

$$t_V = \frac{s_T w_T}{b} + t_{Vw} \quad (39)$$

Summing moments about the line XX gives

$$M_{VT} = [s_T w_T (t - t_V + \frac{1}{2}s_T) + \frac{1}{2}bt_V^2 + bt_{Vw}(t - t_V - \frac{1}{2}t_{Vw})]F_y \quad (40)$$

Equating Eqs. 23 and 40 and substituting for  $t_V$  results in

$$bt_{Vw}^2 + (s_T w_T - bt)t_{Vw} - s_T w_T (t + \frac{1}{2}s_T) + \frac{V_T a}{F_y} + \frac{(s_T w_T)^2}{2b} = 0 \quad (41)$$

which can be solved for  $t_{Vw}$ . Knowing  $t_{Vw}$ ,  $t_V$  is found by Eq. 39 and the thickness of the flange assigned for the axial force,  $P_T$ , is

$$t_P = t - t_V - t_{Vw} \quad (42)$$

The magnitude of the axial force is

$$P_T = bt_P F_y \quad (43)$$

and the corresponding force equal to it in the slab has thickness  $c_{PT}$  as determined by Eq. 37. The moment due to eccentricity is found by summing the moments about the  $NA_P$  which gives

$$M_e = \frac{1}{2}c_{PT}P_T + (c_r - c_{PT} + t_V + \frac{1}{2}t_P)P_T \quad (44)$$

In both cases when the slab is not completely used, the total plastic moment capacity is given by Eq. 30.

High Shear Solution. The second major case, Case II, is called high shear, in which part of the total shear goes to the bottom tee and all the top tee capacity is utilized to resist  $V_T$  and  $M_{VT}$ . Because the capacity of the top tee is used entirely for  $V_T$  and  $M_{VT}$ ,  $M_e$  is zero throughout Case II. To find the capacity for  $V_T$  and  $M_{VT}$  of the top tee, a trial and error method is applied using four equations. The first is the expression for  $w_T$  as given by Eq. 12. The second equation, referring to Fig. 11, gives the thickness of the flange below the  $NA_P$  of the top steel tee as

$$\tau_x = \frac{-s_T w_T + bt}{2b} \quad (45)$$

Equation 23 is the third equation required, and the last one is found by summing moments about the  $NA_p$  in Fig. 11

$$M_{VT1} = [s_T w_T (t_x + \frac{1}{2}s_T) + \frac{1}{2}bt_x^2 + \frac{1}{2}b(t - t_x)^2]F_y \quad (46)$$

Assuming a value of  $V_T$ ,  $M_{VT}$  and  $M_{VT1}$  are calculated and compared and  $V_T$  is adjusted until they are equal, giving the capacity of the top tee for  $V_T$  and  $M_{VT}$ . These values of  $V_T$  and  $M_{VT}$  are constant throughout the high shear case. With the shear assigned to the top tee known, the shear assigned to the bottom tee is

$$V_B = V - V_T \quad (47)$$

and the moment due to shear in the bottom tee is

$$M_{VB} = V_B a \quad (48)$$

Because the bottom tee now has shear assigned to it, it has a reduced web thickness

$$w_B = t_w \sqrt{1 - 3\left(\frac{V_B}{s_B t_w F_y}\right)^2} \quad (49)$$

At this point, the treatment of the bottom tee is very similar to that of the top tee in the low shear case where the  $NA_p$  of the top tee - remaining concrete slab section was in the slab. The calculations are the same for the bottom tee as the top tee in both cases ( $s_V$  greater than or less than  $s_T$ ) to the point where the portions of the tee used for the axial force  $P_B$  are found.

When  $s_V$  is less than  $s_T$ , the axial force is (Fig. 12a)

$$P_B = (s_P w_B + bt_P)F_y \quad (50)$$

The corresponding axial force in the concrete is assigned to the slab

starting at the top and having thickness  $c_{PB}$  as given by Eq. 14. The distance,  $y_c$ , from the top edge of the opening to the line of action of the force  $P_B$  in the concrete is expressed by Eq. 15 and the distance from the bottom edge of the opening to the centroid of the force  $P_B$  in the bottom steel tee is

$$y_B = \frac{\frac{1}{2}s_P^2 w_B + bt_P(s_P + \frac{1}{2}t_P)}{s_P w_B + bt_P} + s_V \quad (51)$$

The moment arm,  $d_c$ , of the forces is determined by Eq. 17, and is used to find the total plastic moment, which is

$$M = P_B d_c \quad (52)$$

because  $M_e$  is zero.

In the other case of  $s_V$  being greater than  $s_T$ , the axial force is (Fig. 12b)

$$P_B = bt_P F_y \quad (53)$$

Again the same force in the concrete is assigned starting at the top of the slab and having thickness  $c_{PB}$ , which is calculated from Eq. 14. The distance  $y_c$  to the line of action of the force  $P_B$  in the concrete from the top edge of the opening is given by Eq. 15, while the distance from the bottom edge of the opening to the centroid of the force  $P_B$  in the bottom steel tee is

$$y_B = s_B + t_{VW} + \frac{1}{2}t_P \quad (54)$$

The moment arm  $d_c$  of the two forces is determined by Eq. 17, and the total moment capacity as before is found using Eq. 52.

#### Calculation of Interaction Diagrams

This section presents the sequence of calculations used in developing

a shear-moment interaction diagram. A broad view of the entire sequence with all cases will be presented first, with the details of each individual case considered later.

Figure 13 is the overall flow diagram of the procedure followed in developing an interaction diagram. First, after input data is read, reference values for a composite beam with known dimensions and material properties are calculated. One limit set on the solution at the outset is that the total axial force capacity of the bottom tee,  $P_B$ , must be less than the total axial force capacity of the concrete slab,  $P_{yc}$ . This limit is used since a composite beam with the force  $P_B$  greater than the force  $P_{yc}$  is an impractical case, and therefore not considered here.

If  $P_B$  is less than  $P_{yc}$ , the input and reference values are printed, after which the total shear,  $V$ , ( $V = V_T$  in Case I) is initialized to zero. The value by which the total shear is incremented is 1.0 and is labeled  $V_{inc}$ . Later, as the interaction diagram is developed, its slope becomes steeper, requiring a smaller increment of shear, i.e.,  $V_{inc} = 0.1$ .

At this point a program control, "check", is also set equal to zero. When "check" is equal to zero, a further decision is needed before going to Case IA or IB. When Case IB is used once, "check" is set equal to one, so that the solution process returns to Case IB.

The next decision deals with the total axial force capacities of the top steel tee and the remaining concrete slab (thickness  $c_r$ ), which are  $P_{yT}$  and  $P_{ycr}$ , respectively. Details of this decision step were discussed in the previous section. After this decision, the solution continues to either Case IA or Case IB, both of which are shown in more detail in Figs. 14 and 15, respectively.

At the end of either case, the required output for the interaction diagram is printed. The value of shear is incremented by  $V_{inc}$  and the

new shear,  $V$ , is compared with the total allowable shear on the top web stub,  $V_{yT}$ . If the value of shear is less than  $V_{yT}$ , then the process is repeated in the appropriate case giving more coordinates for the interaction diagram. The solution is stopped if  $V$  is greater than  $V_{yT}$ , since it is not applicable to failure in shear.

Case IA or Case IB will eventually give way to Case II. Figure 16 is a detailed flow chart of the solution process within Case II. At the end of Case II, data for the interaction diagram is printed after which the shear is increased by  $V_{inc}$ , which is now 0.1. The value of the shear on the bottom tee,  $V_B$ , is now found and compared with the total shear the bottom tee stub will allow,  $V_{yB}$ . If the shear force  $V_B$  is less than  $V_{yB}$ , then Case II is repeated. If  $V_B$  is greater than  $V_{yB}$ , this solution is not applicable and the calculations cease. At the end, enough coordinates will have been computed to plot the entire interaction diagram.

Figure 14 shows the steps involved within Case IA, all of which have been discussed earlier except for the decision of whether  $M_e$  is greater than zero.  $M_e$  must be greater than zero in Case IA by definition, and if it is not Case II takes over. At the end of each cycle through Case IA, the coordinates of the interaction diagram are computed.

Case IB (Fig. 15) is activated when  $P_{yT}$  is less than  $P_{ycr}$  or  $M_{Vmax}$  is less than  $M_{VT}$ . The value of "check" is changed to equal 1.0 so that the Case IA is by-passed through the remainder of the solution. The terms  $A_{sV}$ ,  $B_{sV}$ ,  $C_{sV}$ , and  $Q_{sV}$  deal with the quadratic equation for  $s_V$  (Eq. 33).  $A_{sV}$ ,  $B_{sV}$ , and  $C_{sV}$  are the coefficients, and  $Q_{sV}$  is the portion under the square root of the quadratic. If  $Q_{sV}$  is less than zero, an imaginary number results, so the solution is directed to solve for  $t_{Vw}$  in a manner similar to that for  $s_V$ . If  $Q_{tVw}$  results in an imaginary number, the solution is switched to Case II. If either  $s_V$  or  $t_{Vw}$  are

found, the remaining calculations are performed, and coordinates for the interaction diagram are computed. Again, a check for  $M_e$  is made in Case IB similar to that in Case IA.

Case II (Fig. 16) occurs when  $M_e$  is less than or equal to zero, or when  $Q_{tVw}$  is less than zero. At the beginning  $M_e$  is set equal to zero, the bottom shear to top shear ratio is set equal to zero and the value of shear increment,  $V_{inc}$ , is changed to 0.1 for reasons given earlier. With the given shear ratio,  $V_T$  and  $V_B$  are found and the moments  $M_{VT}$  and  $M_{VT1}$  are computed and compared. Adjustments are made to the shear ratio until  $M_{VT}$  and  $M_{VT1}$  are equal. Then, as in Case IB, calculations and decisions are made concerning  $Q_{sV}$  and  $Q_{tVw}$ . If  $Q_{tVw}$  is less than zero, the solution terminates. Again calculations are made if values for  $s_V$  or  $t_{Vw}$  are found, and the last of the coordinates for the interaction diagram are determined.



## TYPICAL RESULTS AND DISCUSSION

Interaction Diagrams

The computer solution which is shown in Appendix III follows the flow diagrams discussed in the previous chapter, and results in a shear-moment interaction diagram as in Fig. 17. This diagram is the predicted failure envelope for a specific beam of known dimensions and material properties. Shear and moment are non-dimensionalized by the total shear capacity of the gross web section,  $V_p$ , and the total plastic moment capacity of the gross section,  $M_{pC}$ , respectively. For any given set of loading conditions and opening location, the theoretical failure load can be determined.

As indicated in Fig. 17, two possibilities for the top portion of the curve were investigated based on two different methods of distributing the moment due to shear in the top tee. For the bottom curve, Distribution I, the moment due to shear was assigned at the top of the tee section as shown in Fig. 18a. The interaction diagram from this distribution had a rather sharp downward curve at the beginning. For Distribution II (top curve) the moment due to shear was assigned at opposite ends of the top steel tee (Fig. 18b), resulting in a higher moment capacity initially, but ending with a slope discontinuity as the two curves meet at the end of Case I. Because Distribution II gives a higher moment capacity, and it is consistent with the distribution assumed in the bottom tee, it was adopted for this analysis.

The slope discontinuity in the interaction diagram appears to be related to the assignment of the moment due to shear in both steel tees. In Case I the total moment capacity is composed of the primary moment, which is constant, and the moment due to eccentricity,  $M_e$ , which varies.

Because the primary moment is constant it will not bring about a change in the rate of decrease of the total moment in the interaction diagram, whereas  $M_e$  will. The change in  $M_e$  is brought about by several factors, the first of which deals with web thickness. As shear is added in equal increments, the change in web thickness should be at a constant rate thus giving a constant rate of change in the interaction diagram. A second factor is the change in the moment arm of  $M_e$ . At the concrete end, the arm would be increasing as less concrete is used for larger shear loads, while the end in the steel will become shorter. The concrete is not "thrown away" faster than the centroid in the steel moves, so the moment arm for  $M_e$  decreases at a slight rate as shear is increased. Since the magnitude of  $M_e$  gets smaller as its moment arm gets smaller, no considerable change would occur in the slope of the interaction diagram. The final factor deals with the rate at which area of steel is used for  $M_{VT}$  (or  $M_{VB}$ ) as shear is added. At first, a small portion of the top tee is required for  $M_{VT}$  because of a large moment arm, but as more shear is added, more area of steel is used in each increment because of decreasing moment arm length (Fig. 19). This would cause  $M_e$  as well as the total moment to become smaller at an increasing rate, giving an increased rate of change in the slope of the interaction diagram. The slope reaches its steepest point at the end of Case I, after which in Case II the bottom tee is assigned  $M_{VB}$  in the same manner as the top tee, so the slope is fairly flat at first but later gets very steep.

Figure 20 shows a comparison of the interaction diagrams for a non-composite beam and a composite beam. Both curves are for the same W shape and have the same material properties and opening dimensions.

The plot for the non-composite beam was produced using a computer program developed by Scritchfield (9). Because the beams have unequal total plastic moment capacities, the  $M/M_P$  coordinates for the non-composite beam have been multiplied by  $M_P/M_{PC}$  to permit a comparison. Since the composite beam has a higher  $M/M_{PC}$  value, it would appear to be the more effective section. At the lower end of the interaction diagram the two curves coincide, which should be expected since it was assumed that the concrete does not carry any of the shear force.

#### Effects of Varying Key Parameters

A series of interaction diagrams have been prepared to investigate the effect of some of the key parameters. In this parametric study, a W 18x50 beam,  $F_y = 36$  ksi.,  $f'_c = 3.5$  ksi. and a slab width of 48 in. were adopted, while slab thickness and opening length, height and eccentricity were varied one at a time. In the following discussion, an interaction diagram for  $c = 4$  in.,  $h = 4.5$  in.,  $a = 6.75$  in. and  $e = 0$  is common to all of the figures.

When the slab thickness is varied, not much change is effected in the interaction diagram as can be seen in Fig. 21. For each larger thickness, the moment capacity for any value of shear force is increased because of longer moment arms for both  $M_e$  and the primary moment, but the total moment capacity,  $M_{PC}$ , is also increased, resulting in little variation in the  $M/M_{PC}$  ratio. Because  $M_{PC}$  does not increase faster than the moment capacity as larger thicknesses are used, the smaller thicknesses have larger  $M/M_{PC}$  values. All curves meet at the same value of shear, showing that the shear load is independent of the slab thickness, since it is assumed that the slab carries no shear.

Figure 22 shows the variation in the interaction diagram for changes in opening length. With a shear force of zero, all the curves have the same  $M/M_{Pc}$  ratio, which shows that change in opening length does not affect the moment capacity in pure bending. The longer the opening length, the less shear load the beam will withstand. This occurs due to the fact that moments due to shear,  $M_{VT} = V_T a$  and  $M_{VB} = V_B a$ , increase with opening length, thus with a longer opening the steel section is spent more quickly as shear force is increased.

The effect of varying opening height is illustrated by the interaction diagrams in Fig. 23. The smaller the opening height, the greater the  $M/M_{Pc}$  ratio will be, because less of the beam cross section is lost to the opening. Similarly, with the smaller opening height, a larger shear force can be applied to the beam since more of the cross section is left at the opening.

Figure 24 shows the effects on the interaction diagrams due to variation of opening eccentricity (positive eccentricity is upward and negative eccentricity is downward). The largest positive eccentricity gives the highest initial  $M/M_{Pc}$  ratio. This ratio is high because steel that is in the bottom tee will have a larger moment arm than if it were in the top tee. As the eccentricity decreases, the solution remains in Case I longer since more steel is available in the top tee to resist shear. Curves with equal but opposite eccentricity, closely converge toward the bottom portion, suggesting that the shear capacity of the beam is not significantly affected by the direction of eccentricity.

#### Comparison with Experimental Results

Two tests of composite beams with web openings have been performed by Granade (5). An interaction diagram for the beams is shown in Fig. 25,

and the experimental ultimate loads are also plotted. A large discrepancy exists between the theoretical and experimental values of the failure loads. There are several factors which might contribute to this discrepancy; however their effects are uncertain because the test conditions are not described fully.

A small factor to consider would be the manner in which the material properties of the steel and concrete were determined. This factor would cause only minor changes in the interaction diagram. Another small change might occur from the method of loading the beam. If a dynamic loading process were used, a higher ultimate load would occur giving a higher test point on the interaction diagram. A static loading process would give a lower ultimate load. The effect of strain hardening on the test results could have a significant effect. Since the ultimate strength analysis does not take into account the effects of strain hardening, the experimental ultimate loads would have to be adjusted (3) to give a good comparison between theory and experiment.

A final factor concerns one of the key assumptions made in the analysis presented in this report. The assumption states that no shear force will be assigned to the concrete slab. If part of the shear force were assigned to the slab, ultimate loads predicted from the interaction diagram would be much higher.

## CONCLUSIONS

An ultimate strength analysis of composite beams with web openings has been developed based on McCormick's method. This analysis was used to make a comparison with a non-composite beam, and the composite beam was found to be more effective. Ultimate loads based on this solution were also compared with those observed in two laboratory tests. The theoretical results were found to be very conservative in their predictions of the strength of the test beams.

The effect of variation of certain parameters of a composite beam were studied using the analysis. Observations from this study are as follows:

1. Changes in the slab thickness do not affect the interaction diagram to a large extent.
2. The longer the opening is, the smaller the failure load.
3. As the opening is made deeper, the moment and shear capacity decrease.
4. An opening with the highest positive eccentricity has the highest moment capacity.

## RECOMMENDATIONS FOR FURTHER RESEARCH

Further study is needed in regard to the slope discontinuity in the interaction diagram. This study should be directed toward determining if an assignment of forces can be made such that the slope discontinuity is removed. Also, the assignment of shear force to the concrete slab should be considered in future analytical work. The analysis presented in this report could be expanded so that it could be applied to composite beams with reinforcement at the web opening.

More experimental tests on composite beams with web openings would be helpful for comparison with theoretical work.

## ACKNOWLEDGMENTS

The author would like to extend his appreciation to his major professor, Dr. Peter B. Cooper, for his much needed assistance and guidance throughout the development of this thesis.

Thanks also go to the Department of Civil Engineering at Kansas State for financial assistance, and to the National Science Foundation for its support through Grant ENG 76-19045.



## APPENDIX I REFERENCES

1. Bower, J. E., "Ultimate Strength of Beams with Rectangular Holes," Journal of the Structural Division, ASCE, Vol. 94, No. ST6, Proc. Paper 5982, June 1968.
2. Congdon, J. G., and Redwood, R. G., "Plastic Behavior of Beams with Reinforced Holes," Journal of the Structural Division, ASCE, Vol. 96, No. ST9, Proc. Paper 7561, Sept. 1970.
3. Cooper, P. B., Snell, R. R., and Knostman, H. D., "Failure Tests on Beams with Eccentric Web Holes," Journal of the Structural Division, ASCE, Vol. 103, No. ST9, Proc. Paper 13203, Sept. 1977.
4. Frost, R. W., "Behavior of Steel Beams with Eccentric Web Holes," Technical Report 46.019-400(1), Applied Research Laboratory, United States Steel Corporation, Feb. 1973.
5. Granade, C. J., "An Investigation of Composite Beams Having Large Rectangular Openings in Their Webs," thesis presented to the University of Alabama, at University, Ala., in 1968, in partial fulfillment of the requirements for the degree of Master of Science.
6. McCormick, M. M., "Open Web Beams-Behavior Analysis and Design," Melbourne Research Laboratories, Report MRL 17/18, Clayton, Victoria, Australia, Feb. 1972.
7. Redwood, R. G., "The Strength of Steel Beams with Unreinforced Web Holes," Civil Engineering and Public Works Review, Vol. 64, No. 755, London, June 1969.
8. Richard, M. W., "Ultimate Strength Analysis of Beams with Eccentric Rectangular Web Openings," thesis presented to Kansas State University, at Manhattan, Kan., in 1971, in partial fulfillment of the requirements for the degree of Master of Science.
9. Scritchfield, R. G., "Ultimate Strength Predictions for Beams with Web Openings," thesis presented to Kansas State University, at Manhattan, Kan., in 1975, in partial fulfillment of the requirements for the degree of Master of Science.
10. Seely, F. B., and Smith, J. O., "Stresses and Strains at a Point. Theories of Failure by Yielding," Advanced Mechanics of Materials, 2nd ed., John Wiley and Sons, Inc., New York, N.Y., 1952, pp. 69-91.
11. "Specification for the Design, Fabrication and Erection of Structural Steel for Buildings," American Institute of Steel Construction, 7th ed., New York, 1973.
12. Wang, T. M., Snell, R. R., and Cooper, P. B., "Strength of Beams with Eccentric Reinforced Holes," Journal of the Structural Division, ASCE, Vol. 101, No. ST9, Proc. Paper 11540, Sept. 1975.

## APPENDIX II NOTATION

- $a$  - one-half length of opening  
 $b$  - width of steel flange  
 $b_c$  - width of concrete slab  
 $c$  - thickness of concrete slab  
 $c_{PB}$  - thickness of concrete used to equal axial force  $P_B$   
 $c_{Ps}$  - thickness of concrete used to equal axial force  $P_{ys}$   
 $c_{PT}$  - thickness of concrete used to equal axial force  $P_T$   
 $c_r$  - thickness of concrete left after thickness  $c_{PB}$  due to  $P_B$  is subtracted from original thickness  $c$   
 $d$  - depth of steel section  
 $d_c$  - moment arm between axial force in bottom tee and corresponding force in slab  
 $d_e$  - moment arm between axial force in top tee and corresponding force in slab  
 $e$  - eccentricity of opening  
 $F_c$  -  $.85 f'_c$   
 $f'_c$  - compressive strength of concrete cylinder  
 $F_y$  - yield stress of steel  
 $h$  - one-half opening depth  
 $M$  - total moment capacity of beam at centerline of opening  
 $M_{cap}$  - total moment capacity of top tee-concrete slab ( $c_r$ ) section  
 $M_e$  - moment due to eccentricity  
 $M_p$  - total moment capacity of non-composite beam without opening  
 $M_{Pc}$  - total moment capacity of composite beam without opening  
 $M_{VB}$  - moment due to shear in bottom tee

- $M_{Vmax}$  - maximum  $M_{VT}$  allowed in top tee due to location of  $NA_p$   
 $M_{VT}$  - moment due to shear in top tee  
 $M_{VT1}$  - value of  $M_{VT}$  for any value of shear by  $\Sigma$  Moments - used to compare with value  $M_{VT}$   
 $P_B$  - axial force in bottom tee which contributes to primary moment  
 $P_T$  - axial force in top tee which contributes to  $M_e$   
 $P_{yc}$  - total axial force capacity of concrete slab  
 $P_{ycr}$  - axial force of concrete slab remaining after  $c_{PB}$  removed  
 $P_{ys}$  - total axial force capacity of steel section at opening  
 $P_{yT}$  - axial force of top steel tee with web reduced for shear  
 $s_B$  - depth of web section in bottom tee at opening  
 $s_P$  - depth of web assigned to axial force  $P_B$  or  $P_T$   
 $s_T$  - depth of web section in top tee at opening  
 $s_V$  - depth of web assigned to axial force component of  $M_{VT}$  or  $M_{VB}$   
 $t$  - steel flange thickness  
 $t_P$  - thickness of flange assigned to axial force  $P_B$  or  $P_T$   
 $t_t$  - thickness of top steel flange below  $NA_p$  of composite beam without opening  
 $t_V$  - thickness of outside edge of flange assigned to  $M_{VT}$  or  $M_{VB}$   
 $t_{Vw}$  - thickness of flange adjacent to web assigned to  $M_{VT}$  or  $M_{VB}$   
 $t_w$  - steel web thickness  
 $t_x$  - thickness of top flange in tension below  $NA_p$   
 $V$  - total shear applied to composite beam web with opening  
 $V_B$  - shear assigned to bottom tee

$V_p$  - total shear capacity of web of steel section with no opening

$V_T$  - shear assigned to top tee

$V_{yB}$  - total shear capacity of web of bottom tee section at opening

$V_{yT}$  - total shear capacity of web of top tee section at opening

$w_B$  - reduced web thickness for bottom tee

$w_T$  - reduced web thickness for top tee

$y$  - distance from bottom of web of top tee section to the  $NA_p$  of top tee-concrete slab ( $c_r$ ) section

$y_B$  - distance from top of web of bottom tee to centroid of portion assigned to axial force  $P_B$

$y_c$  - distance from bottom of web of top tee to centroid of slab thickness  $c_{pB}$  used to resist force  $P_B$

## APPENDIX III COMPUTER PROGRAM

```

5JOB
1 REAL H,MC,FP,MF,MPPC,MPC,MVE,MVMAX,MVT,MVTONE
2 READ(5,1) NRM
3
4 1 FORMAT(151)
5 DO 2000 J=1,NBM
6 CHECK=CHECKA=CHECKB=CHECKC=CHECKD=CHECKE=CHECKF=CHECKG=0
7 2 FORMAT(5F7.3,6F6.2)
8 ST=D/2.-C-M-T
9 SB=D/2.+E-B-T
10 VYT=ST*TW*FY/SQRT(3.)
11 VYB=SB*TW*FY/SQRT(3.)
12 VP=TW*(D-2.*T)*FY/SCRT(3.)
13 FC=0.85*FPC
14 PYC=FC*BC*C
15 PYS=FY*(2.*B*T+D-2.*T)*TW
16 IF(PYC .LT. PYS)GO TO 3
17 CPS=PYS/FC*BC*C
18 MPC=FC*(BC*CPS**2/2.-1)+PYS*(D/2.+C-CPS)
19 GO TO 4
20 3 TT=(FC*BC*C-FY*TW*(D-2.*T))/(2.*FY*B)
21 MPC=FC*(BC*C*(C/2.+T-TT)+FY*(1-TT)**2*B/2.+(TT)**2*B/2.+TW*(D-2.*T)*(D/2.-T+TT)+T*B*(D-3.*T/2.+TT))
22 4 PB=FY*(B*T+SB*TW)
23 IF(PB .LT. PYC)GO TO 6
24 WRITE(6,5)
25 5 FORMAT(2X,14)SINCE THE AXIAL YIELD FORCE IN THE BUTTCH TEE IS GRE
LATER THAN THE AXIAL FORCE CAPACITY OF THE CONCRETE SLAB, THIS SOLU
TION IS NOT APPLICABLE.1
26 GO TO 2000
27 6 WRITE(6,7) P,C,T,Th,BC,E,H,A,FY,C,FPC
28 7 FORMAT(1H0,6X,1HE,9X,1HD,9X,1HT,9X,2HTW,7X,2HBC,9X,1FE,9X,1HM,9X,1
CHA,8X,2HEY,5X,1HC,8X,3HEPC,///1E1G,3,/)
29 WRITE(6,B) ST,SB,VYT,VYB,VP,MPC
30 8 FORMAT(1H0,10X,2HST,13X,2HSB,12X,3HVRT,12X,3HVEE,13X,2HVP,11X,3HMP
CC,///6F15.3,/)
31 WRITE(6,9)
32 9 FORMAT(1H0,10X,1HV,13X,5HVB/VT,11X,2HDC,12X,1HP,15X,2HME,12X,4HV/V
CP,11X,5HM/MPC)
33 V=VT=0
34 VBT=0
35 VIAC=1.0
36 10 WT=TW*SQRT(1.-3.*(VT/1ST*TW*FY)**2)
37 CPB=PB/(DC*FC)
38 YC=ST+T+C-CPB/2.
39 YB=(1./(SB*TW*B*T))*(SB**2*TW/2.+B*T*(SB+T/2.))
40 DC=YR+H**2.+YC
41 CR=C-CPB
42 PYC=FC*BC*CR
43 PYT=FY*(B*T+ST*WT)
44 MVT=VTA
45 IF(CHECK .EQ. 1.) GO TO 27
46 IF(CHECKA .EQ. 1.)GO TO 15
47 IF(PYB .LT. PYT)GO TO 13
48 11 WRITE(6,12)
49 12 FORMAT(1H0,40)PYCR IS GREATER THAN PYT. GO TO CASE IB.1
50 GO TO 27
51 13 WRITE(6,14)
52 14 FORMAT(1H0,37)PYCR IS LESS THAN PYT. GO TO CASE IA.)
53 CHECKA=1

```

54	15	$Y=ST+T/2.-ST*WT/(2.*B)+(FC/FY)*(CP*BC/(2.*B))$
55		$NCAP=FY*(ST*WT*(Y-ST/2.)+B/2.*(Y-ST)**2+3/2.*(ST+T-Y)**2)+CR*BC*(S$ $C)+T-Y+CR/2.)*FC$
56		$TV=ST+T-Y$
57		$SV=TV*B/WT$
58		$IF(SV.GT.ST)IGC TC 17$
59		$MVMAX=TV*B*(ST+T-TV/2.-SV/2.)*FY$
60		$IF(CHECKB.EC.1.)GO TO 19$
61		$WRITE(6,16)$
62	16	FORMAT(1H0,4X,24HME EXTENDS INTO THE WEB.)
63		CHECKB=1
64		GO TO 19
65	17	$TVW=(TV*B-ST*WT)/B$
66		$MVMAX=(TV**2/2.*P+TVW*B*(T-TVW/2.-TV))+ST*WT*(Y-ST/2.)*FY$
67		$IF(CHECKC.EC.1.)GO TO 19$
68		$WRITE(6,18)$
69	18	FORMAT(1H0,4X,24HME IS CONFINED TO THE FLANGE.)
70		CHECKC=1
71	19	$IF(MVMAX.GT.MVT)IGC TO 21$
72		$WRITE(6,20)$
73	20	FORMAT(1H0,30HMOVMAX IS LESS THAN MVT, GO TO CASE 1B.)
74		GO TO 27
75	21	$ME=NCAP*MVT$
76	22	$IF(ME.GT.0.)GO TO 24$
77		$WRITE(6,23)$
78	23	FORMAT(1H0,36HME IS LESS THAN ZERC, GO TO CASE 11.)
79		GO TO 33
80	24	$M=PB*DC*ME$
81		$VVP=V/VP$
82		$MMPC=M/MPC$
83		$WRITE(6,25) V,VRT,DC,M,ME,VVP,MMPC$
84	25	FORMAT(7F15.4)
85		$V=VT+V*VINC$
86		$IF(VT.LT.VT)IGC TO 10$
87		$WRITE(6,26)$
88	26	FORMAT(1H0,6)WHEN VT IS GREATER THAN VY, THIS SOLUTION IS NOT AP PLICABLE.)
89		GO TO 2000
90	27	CHECK=1
91		$ASV=.5*WT/(2.*B)$
92		$BSV=-(ST+T)$
93		$CSV=V*A/(hT*FY)$
94		$OSV=RSV**2-4.*ASV*CSV$
95		$IF(OSV.LT.0.)GO TO 29$
96		$SV=(-OSV-SCTP(0SV))/(-2.*ASV)$
97		$IF(SV.GT.ST)IGC TC 29$
98		$TV=SV*WT/B$
99		$SP=ST-SV$
100		$TP=T-TV$
101		$P1=FY*(TP*D+SP*WT)$
102		$CPT=PT*(BC*FC)$
103		$MF=(BC*CP**2/2.)*FC*(SP*WT*(CR-CPT+T*SP/2.))+TP*B*(CR-CPT+TV*TP/2.$ $C)*FY$
104		$IF(CHECKD.EC.1.)GO TC 22$
105		$WRITE(6,28)$
106	28	FORMAT(1H0,4X,44HSV IS LESS THAN ST; ME EXTENDS INTO THE WEB.)
107		CHECKD=1
108		GO TO 22
109	29	$ATV=M/P$
110		$RTVh=-(ST*WT-B*AT)$

```

111      CTVM=-ST*WT*(T+ST/2.)*V*A/FY+(ST*WT)**2/(2.*B)
112      QTVM=LRTVM**2)-4.*ATVM*CTVM
113      IF(QTVM.GT. 0.1)GO TO 31
114      WRITE(6,30)
115      30 FORMAT(1H0,60HSQUARE ROOT IN QUADRATIC FOR TVM IS NEGATIVE, GO TO
        ICASE 11.)
116      GO TO 33
117      31 TVM=(LRTVM-SQRT(QTVM))/(2.*ATVM)
118      TV=(ST*WT)/R*ATVM
119      TP=T-TV*V
120      PT=TP*B*FY
121      CPT=PT/(BC*FC)
122      ME=CPT*PT/2.*ICR-CPT*TV*TP/2.1*PT
123      IF(CHECKE .EC. 1.1)GO TO 22
124      WRITE(6,32)
125      32 FORMAT(1H0,4X,52HVS IS GREATER THAN ST; HE IS CNFINED TO THE PLAN
        IGE.)
126      CHECKE=1
127      GO TO 22
128      33 ME=0
129      VBT=0
130      34 VT=V/(1.+VBT)
131      VB=V-VT
132      IF(VT.LT. VBT)IGC TO 35
133      VBT=VBT+.001
134      GO TO 34
135      35 IF(VB.LT. VBT)IGD TO 36
136      VBT=VBT+.001
137      GO TO 34
138      36 WT=TW/SQRT(1.-3.*(VT/(ST+TW*FY))**2)
139      TX=(R*T-ST*WT)/(2.*B)
140      MVT=VT*A
141      MVTONE=(1-TX)**2*B/2.+B*TX**2/2.+ST*WT*(TX*ST/2.)*FY
142      IF(MVTONE.GT. MVT)IGC TO 38
143      VBT=VBT+.0001
144      GO TO 34
145      37 VBT=VB/VT
146      MVB=VA*A
147      38 WR=TW/SQRT(1.-3.*(VB/(SB+TW*FY))**2)
148      ASV=.5*WR/(2.*B)
149      PSV=-1SD*1
150      CSV=VSB*ASV/FY
151      OSV=BSV**2-4.*ASV*CSV
152      IF(OSV.LT. 0.1)IGC TO 40
153      SV=-PSV-SQRT(CSV)/2.*ASV)
154      IF(SV.GT. SB)IGD TO 43
155      TV=SV*WB/B
156      TP=T-TV
157      SP=SB-SV
158      PB=FY*(SP*WB+TP*B)
159      YE=(TP*B-(SP*TP/2.)*SP**2*WB/2.)/(SP*WB+TP*B)+SV
160      IF(CHECKF .ED. 1.1)GO TO 44
161      WRITE(6,34)
162      39 FORMAT(1H0,4X,64HVS IS LESS THAN SB; PB EXTENDS INTO THE WEB.)
163      CHECKF=1
164      GO TO 44
165      43 ATVM=B
166      RTVM=(SB*WB-B*T)
167      CTVM=-SR*WB*(T+SR/2.)*V*B*A/FY+(SB*WB)**2/(2.*B)
168      QTVM=LRTVM**2)-4.*ATVM*CTVM

```

```

169 IF(CTV# .GT. 0.1GC TC 42
170 WRITE(6,41)
171 41 FORMAT(1P0.5SHSQUARE ROOT IN THE QUADRATIC FOR TV# IS NEGATIVE, ST
TOP
172 GO TO 2330
173 42 TV#=(8IV#-SQR(8IV#**2-4*ATV#))
174 TV#=(S0*W3)/B+IV#
175 TP=T-TV-TV#
176 PR=TP*B*FV
177 Y0=S0+TV#*TP/2.
178 IF(CHECKG .EQ. 1.1GC TC 44
179 WRITE(6,43)
180 43 FORMAT(140.4X,52MSV IS GREATER THAN SB; P3 IS CENFIAC TO THE FLAN
1GF.)
181 CHECKG=1
182 44 VINC=3.1
183 CP=P*B/(1C+FC)
184 YC=ST+1C-CPR/2.
185 DC=Y3+2.*M*YC
186 M=PD*DC
187 VVP=V/VP
188 MNP=V/MPC
189 WRITE(6,45) V.VBT,DC,M,ME,VVP,MNP
190 45 FORMAT(7F15.4)
191 V=V+VINC
192 VR=V-VT
193 IF(V3 .LT. VVB)GO TO 37
194 WRITE(6,46)
195 46 FORMAT(11H).61HWHEN VB IS GREATER THAN VVB, THIS SCLUTICA IS NOT AP
1P(CABLE.)
196 2000 CONTINUE
197 STOP
198 END

```

## SENTRY

B	D	T	TW	DC	E	M	A	FY	C	FPC
7.500	18.200	0.970	7.358	48.000	0.070	6.500	6.750	36.030	4.300	3.530

ST	SB	VVT	VVB	VP	MPC
3.930	3.930	29.243	29.243	125.483	566C.773

V	VB/VT	GC	M	PE	V/VP	M/MPC
---	-------	----	---	----	------	-------

PCB IS GREATER THAN PYT, GO TO CASE 1F.

SV IS LESS THAN ST; HE EXTENDS INTO THE WEB.

0.0000	0.0000	20.4416	4722.2650	550.9551	0.0000	0.6075
1.0000	0.3333	20.4416	4721.9333	543.6316	0.3380	0.6057
2.0000	0.3300	20.4416	4711.1670	525.8369	0.0159	0.8038
3.0000	0.3033	20.4416	4694.5720	510.4431	0.0239	0.6019
4.0000	0.3033	20.4416	4688.1160	506.5896	0.0319	0.7999
5.0000	0.0000	20.4416	4676.1560	494.6262	0.0399	0.7979
6.0000	0.0000	20.4416	4663.4530	482.1228	0.0478	3.7557



7.0000	0.0000	20.4416	4650.1440	46E.8159	0.C558	0.7934
8.0700	0.0000	20.4416	4636.1600	454.8291	J.0638	J.7913
9.0700	0.0000	20.4416	4621.3600	44C.C558	J.0717	0.7885
10.0000	0.0000	20.4416	4605.6950	424.3033	J.C797	0.7859
11.0000	J.1333	21.4416	4588.9590	421.5286	J.C677	0.7830
12.0000	0.0000	20.4416	4570.5460	369.2168	0.C957	0.7799
13.0000	0.0000	20.4416	4553.1640	368.6323	0.1236	0.7764
14.0000	J.1333	21.4416	4526.4410	345.1118	J.1116	C.7723
15.0000	0.0000	20.4416	4495.5030	314.1736	C.1196	0.7670
SV IS GREATER THAN ST: WE IS CONFINED TO THE FLANGE.						
16.0000	0.0000	20.4416	4418.9170	237.5891	0.1275	0.7540
SQUARE ROOT IN QUADRATIC FCP TWM IS NEGATIVE, GO TO CASE II.						
SV IS LESS THAN SB: PB EXTENDS INTO THE WEB.						
17.0000	0.0106	20.4472	4171.4680	C.C000	0.1355	0.7118
17.1330	0.2165	21.4574	4165.9293	J.1333	J.1363	0.7128
17.2000	0.0225	20.4535	4160.3430	C.C000	0.1371	0.7099
17.3000	0.1284	20.4567	4154.7260	0.C000	0.1379	0.7089
17.4000	J.1364	21.4559	4149.3820	J.C000	0.1387	0.7079
17.5000	0.0403	20.4631	4143.4060	C.C000	0.1395	0.7070
17.5995	0.0463	20.4663	4137.7070	0.C000	0.1403	0.7060
17.6995	0.2522	20.4695	4131.9760	C.C000	0.1411	C.7050
17.7995	0.0582	20.4728	4126.2140	C.C000	J.1419	C.7040
17.8995	0.0641	20.4763	4120.4290	J.1333	J.1427	0.7031
17.9995	0.0700	20.4793	4114.6050	C.C000	0.1435	0.7021
18.0995	0.0760	20.4826	4108.7570	0.C000	0.1443	0.7011
18.1995	J.0819	20.4859	4102.8820	J.1333	0.1451	0.7001
18.2995	0.0879	20.4892	4096.9720	C.C000	0.1459	0.6990
18.3995	0.0938	20.4925	4091.1330	C.C000	J.1467	J.6980
18.4995	J.0998	20.4959	4085.0630	C.C000	J.1475	0.6970
18.5995	0.1057	20.4992	4079.0020	C.C000	C.1483	0.6960
18.6995	0.1116	20.5026	4073.3290	J.1333	J.1491	J.6950
18.7995	0.1176	20.5060	4066.9680	C.C000	0.1499	0.6939
18.8995	0.1235	20.5094	4060.8730	C.C000	0.1507	C.6929
18.9995	J.1295	20.5128	4054.7470	J.1333	0.1514	0.6918
19.0995	0.1354	20.5163	4048.5680	C.C000	0.1522	0.6908
19.1995	0.1414	20.5197	4042.3980	C.C000	J.1530	J.6897
19.2995	J.1473	20.5232	4036.1740	C.C000	0.1538	0.6887
19.3995	0.1533	20.5266	4029.9130	C.C000	0.1546	0.6876
19.4995	0.1592	20.5302	4023.6310	J.1333	0.1554	J.6865
19.5995	0.1651	20.5337	4017.3050	C.C000	0.1562	0.6855
19.6995	0.1711	20.5372	4010.9520	C.C000	0.1570	0.6844
19.7995	J.1770	20.5407	4004.5650	J.1333	0.1578	0.6833
19.8995	0.1830	20.5443	3998.1400	C.C000	0.1586	0.6822
19.9995	0.1889	20.5479	3991.6850	C.C000	J.1594	J.6811
20.0995	0.1949	20.5515	3985.1940	C.C000	0.1602	0.6800
20.1995	0.2008	20.5551	3978.6640	C.C000	0.1611	0.6789
20.2995	0.2068	20.5587	3972.1340	J.1333	J.1618	0.6777
20.3995	0.2127	20.5624	3965.5050	C.C000	0.1626	0.6766
20.4995	0.2186	20.5660	3958.8740	J.0000	0.1634	0.6755
20.5995	0.2246	21.5697	3952.2320	J.1333	0.1642	0.6743
20.6995	0.2305	20.5734	3945.4570	C.C000	0.1650	0.6732
20.7995	0.2365	20.5771	3938.7540	J.0000	J.1658	J.6721
20.8995	J.2424	20.5807	3931.9740	C.C000	0.1666	0.6709
20.9995	0.2484	20.5844	3925.1570	C.C000	0.1674	0.6697
21.0995	0.2543	20.5882	3918.2990	0.1333	0.1682	0.6686
21.1995	0.2603	20.5920	3911.4040	C.C000	0.1690	0.6674
21.2995	0.2662	20.5960	3904.4720	C.0000	0.1698	0.6662

21.3996	0.2721	20.5998	3897.5000	C.0000	0.1706	0.6650
21.4996	0.2781	20.6037	3899.4870	0.0030	0.1714	0.6638
21.5996	0.2840	20.6075	3883.4340	C.0000	0.1722	0.6626
21.6996	0.2900	20.6114	3876.3400	0.0000	0.1730	0.6614
21.7996	0.2959	20.6153	3869.2060	0.0030	0.1738	0.6602
21.8996	0.3019	20.6192	3862.0310	C.0000	0.1746	0.6590
21.9995	0.3078	20.6232	3854.8150	C.0000	0.1754	0.6577
22.0995	0.3138	20.6271	3847.5540	C.0000	0.1762	0.6565
22.1995	0.3197	20.6311	3840.2510	C.0000	0.1770	0.6552
22.2995	0.3256	20.6351	3832.9060	0.0030	0.1778	0.6540
22.3995	0.3316	20.6391	3825.5130	C.0000	0.1785	0.6527
22.4995	0.3375	20.6432	3818.0790	0.0000	0.1793	0.6515
22.5995	0.3435	20.6473	3810.6010	0.0030	0.1801	0.6502
22.6995	0.3494	20.6514	3803.0750	C.0000	0.1809	0.6489
22.7995	0.3554	20.6555	3795.5030	0.0000	0.1817	0.6476
22.8995	0.3613	20.6596	3787.8820	0.0000	0.1825	0.6463
22.9995	0.3672	20.6637	3780.2180	C.0000	0.1833	0.6450
23.0994	0.3732	20.6679	3772.5230	0.0030	0.1841	0.6437
23.1994	0.3791	20.6721	3764.7410	C.0000	0.1849	0.6424
23.2994	0.3851	20.6763	3756.9260	0.0000	0.1857	0.6410
23.3994	0.3910	20.6806	3749.0630	0.0030	0.1865	0.6397
23.4994	0.3970	20.6848	3741.1510	C.0000	0.1873	0.6383
23.5994	0.4029	20.6891	3733.1820	0.0000	0.1881	0.6370
23.6994	0.4089	20.6934	3725.1650	C.0000	0.1889	0.6356
23.7994	0.4148	20.6978	3717.0940	C.0000	0.1897	0.6342
23.8994	0.4207	20.7021	3708.9680	0.0030	0.1905	0.6328
23.9994	0.4267	20.7065	3700.7870	C.0000	0.1913	0.6315
24.0993	0.4326	20.7109	3692.5500	0.0000	0.1921	0.6300
24.1993	0.4386	20.7153	3684.2560	0.0030	0.1929	0.6286
24.2993	0.4445	20.7198	3675.9030	C.0000	0.1937	0.6272
24.3993	0.4505	20.7243	3667.4940	0.0000	0.1945	0.6258
24.4993	0.4564	20.7288	3659.0260	C.0000	0.1953	0.6243
24.5993	0.4624	20.7333	3650.4950	C.0000	0.1961	0.6229
24.6993	0.4683	20.7379	3641.9020	0.0030	0.1969	0.6214
24.7993	0.4742	20.7425	3633.2440	C.0000	0.1977	0.6199
24.8993	0.4802	20.7471	3624.5260	0.0000	0.1985	0.6184
24.9993	0.4861	20.7517	3615.7410	0.0030	0.1993	0.6169
25.0993	0.4921	20.7564	3606.8890	C.0000	0.2001	0.6154
25.1992	0.4980	20.7611	3597.9700	0.0000	0.2009	0.6139
25.2992	0.5040	20.7658	3588.9820	C.0000	0.2017	0.6124
25.3992	0.5099	20.7706	3579.9240	C.0000	0.2025	0.6108
25.4992	0.5159	20.7754	3570.7540	0.0030	0.2033	0.6093
25.5992	0.5218	20.7802	3561.5880	C.0000	0.2041	0.6077
25.6992	0.5277	20.7850	3552.3100	0.0000	0.2049	0.6061
25.7992	0.5337	20.7899	3542.9560	0.0030	0.2056	0.6045
25.8992	0.5396	20.7948	3533.5210	C.0000	0.2064	0.6029
25.9992	0.5456	20.7998	3524.0070	0.0000	0.2072	0.6013
26.0992	0.5515	20.8047	3514.4110	C.0000	0.2080	0.5996
26.1992	0.5575	20.8097	3504.7330	C.0000	0.2088	0.5980
26.2991	0.5634	20.8148	3494.9680	0.0030	0.2096	0.5963
26.3991	0.5694	20.8199	3485.1180	C.0000	0.2104	0.5947
26.4991	0.5753	20.8250	3475.1770	0.0000	0.2112	0.5930
26.5991	0.5812	20.8301	3465.1440	0.0030	0.2120	0.5912
26.6991	0.5872	20.8353	3455.0150	C.0000	0.2128	0.5895
26.7991	0.5931	20.8405	3444.7900	0.0000	0.2136	0.5878
26.8991	0.5991	20.8457	3434.4670	0.0000	0.2144	0.5860
26.9991	0.6050	20.8510	3424.0410	C.0000	0.2152	0.5842
27.0991	0.6110	20.8564	3413.5100	0.0000	0.2160	0.5824
27.1991	0.6169	20.8617	3402.8740	C.0000	0.2168	0.5806
27.2991	0.6228	20.8671	3392.1250	0.0000	0.2176	0.5788

27.3990	0.6288	20.8726	3381.2640	C.0000	0.2184	0.5769
27.4990	0.6347	20.8781	3370.2860	C.0000	0.2192	0.5751
27.5990	0.6407	20.8836	3359.1860	C.0000	0.2200	0.5732
27.6990	0.6466	20.8892	3347.9620	C.0000	0.2208	0.5712
27.7990	0.6526	20.8948	3336.6100	C.0000	0.2216	0.5693
27.8990	0.6585	20.9004	3325.1240	C.0000	0.2224	0.5674
27.9990	0.6645	20.9061	3313.5020	C.0000	0.2232	0.5654
28.0990	0.6704	20.9119	3301.7380	C.0000	0.2240	0.5634
28.1990	0.6763	20.9177	3289.8280	C.0000	0.2248	0.5613
28.2990	0.6823	20.9235	3277.7670	C.0000	0.2256	0.5593
28.3990	0.6882	20.9294	3265.5470	C.0000	0.2264	0.5572
28.4990	0.6942	20.9354	3253.1650	C.0000	0.2272	0.5551
28.5990	0.7001	20.9414	3240.6120	C.0000	0.2280	0.5529
28.6990	0.7061	20.9474	3227.8850	C.0000	0.2288	0.5508
28.7990	0.7120	20.9535	3214.9720	C.0000	0.2296	0.5486
28.8990	0.7180	20.9597	3201.8680	C.0000	0.2304	0.5463
28.9990	0.7239	20.9659	3188.5660	C.0000	0.2312	0.5441
29.0990	0.7298	20.9722	3175.0550	C.0000	0.2319	0.5417
29.1990	0.7358	20.9785	3161.3270	C.0000	0.2327	0.5394
29.2990	0.7417	20.9850	3147.3710	C.0000	0.2335	0.5370
29.3990	0.7477	20.9914	3133.1760	C.0000	0.2343	0.5346
29.4990	0.7536	20.9980	3118.7330	C.0000	0.2351	0.5321
29.5990	0.7596	21.0046	3104.0210	C.0000	0.2359	0.5296
29.6990	0.7655	21.0113	3089.0330	C.0000	0.2367	0.5271
29.7990	0.7715	21.0180	3073.7500	C.0000	0.2375	0.5245
29.8990	0.7774	21.0249	3058.1600	C.0000	0.2383	0.5218
29.9990	0.7833	21.0318	3042.2390	C.0000	0.2391	0.5191
30.0990	0.7893	21.0388	3025.9640	C.0000	0.2399	0.5163
30.1990	0.7952	21.0459	3009.3230	C.0000	0.2407	0.5135
30.2990	0.8012	21.0532	2992.2820	C.0000	0.2415	0.5106
30.3990	0.8071	21.0603	2974.8120	C.0000	0.2423	0.5076
30.4990	0.8131	21.0677	2956.8870	C.0000	0.2431	0.5045
30.5990	0.8190	21.0751	2938.4700	C.0000	0.2439	0.5014
30.6990	0.8249	21.0827	2919.5160	C.0000	0.2447	0.4981
30.7990	0.8309	21.0904	2899.9810	C.0000	0.2455	0.4948
30.8990	0.8368	21.0983	2879.8160	C.0000	0.2463	0.4914
30.9990	0.8428	21.1062	2858.9540	C.0000	0.2471	0.4878
31.0990	0.8487	21.1143	2837.3240	C.0000	0.2479	0.4841
31.1990	0.8547	21.1226	2814.8420	C.0000	0.2487	0.4803
31.2990	0.8606	21.1310	2791.4040	C.0000	0.2495	0.4763
31.3990	0.8666	21.1396	2766.8860	C.0000	0.2503	0.4721
31.4990	0.8725	21.1484	2741.1350	C.0000	0.2511	0.4677
31.5990	0.8784	21.1574	2713.9560	C.0000	0.2519	0.4631
31.6990	0.8844	21.1667	2685.1060	C.0000	0.2527	0.4581
31.7990	0.8903	21.1763	2654.2550	C.0000	0.2535	0.4529
31.8990	0.8963	21.1861	2620.9480	C.0000	0.2543	0.4472
31.9990	0.9022	21.1964	2584.5470	C.0000	0.2551	0.4410
32.0990	0.9082	21.2072	2544.0620	C.0000	0.2559	0.4341
32.1990	0.9141	21.2186	2497.6480	C.0000	0.2567	0.4262
32.2990	0.9201	21.2309	2442.1270	C.0000	0.2575	0.4168
32.3990	0.9260	21.2449	2377.7480	C.0000	0.2583	0.4045
SV IS GREATER THAN SB: PR IS CONFINED TO THE FLANGE.						
32.4990	0.9319	21.2608	2277.0490	C.0000	0.2590	0.3885
32.5990	0.9379	21.2775	2178.4940	C.0000	0.2598	0.3717
32.6990	0.9438	21.2951	2074.7490	C.0000	0.2606	0.3540
32.7990	0.9498	21.3136	1964.5890	C.0000	0.2614	0.3353
32.8990	0.9557	21.3333	1848.0790	C.0000	0.2622	0.3153
32.9990	0.9617	21.3544	1722.5870	C.0000	0.2630	0.2939
33.0990	0.9676	21.3772	1586.9260	C.0000	0.2638	0.2707

33.1985	0.9736	21.4023	1436.4860	0.0000	0.2646	0.2451
33.2985	0.9795	21.4304	1267.8270	0.0000	0.2654	0.2163
33.3985	0.9854	21.4629	1071.5860	0.0000	0.2662	0.1828
33.4985	0.9914	21.5031	828.0381	0.0000	0.2670	0.1413
33.5985	0.9973	21.5622	467.6882	0.0000	0.2678	0.0798

SQUARE ROOT IN THE QUADRATIC FOR TV% IS NEGATIVE, STOP.

CORE USAGE      OBJECT CODE= 10448 BYTES, ARRAY AREA=      0 BYTES, TOTAL AREA AVAILABLE= 159840 BYTES

DIAGNOSTICS      NUMBER OF ERRORS=      0. NUMBER OF WARNINGS=      0. NUMBER OF EXTENSIONS=      9

COMPILE TIME=      0.61 SEC, EXECUTION TIME=      0.63 SEC.      14.31.13      FRIDAY      28 JUL 78      WATFIV

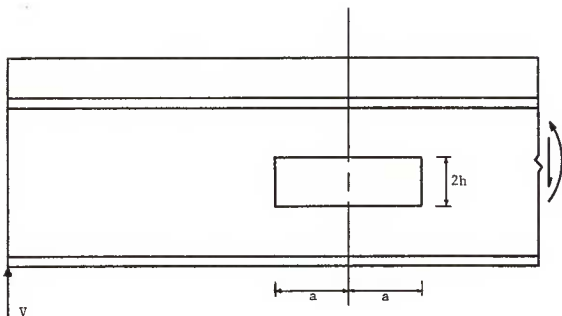


Fig. 1 Elevation of Composite Beam with Web Opening

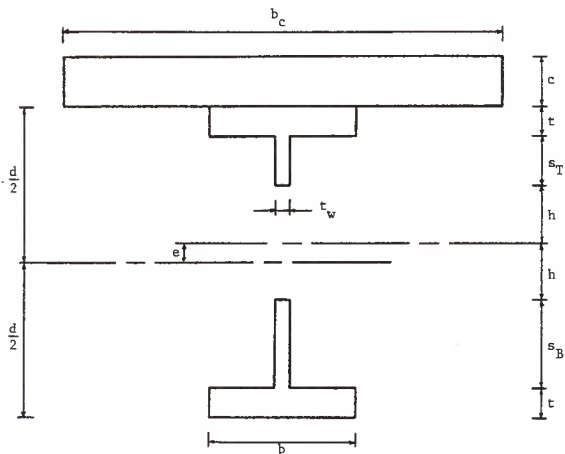


Fig. 2 Section of Composite Beam with Web Opening

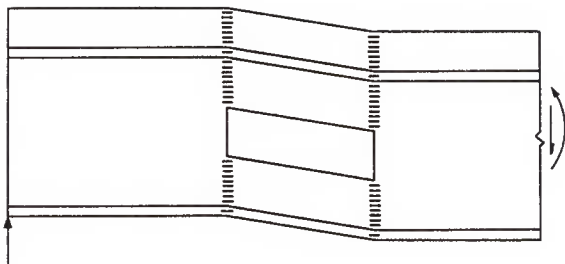
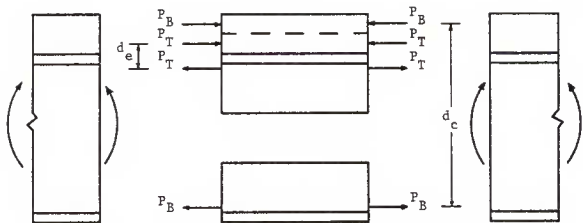
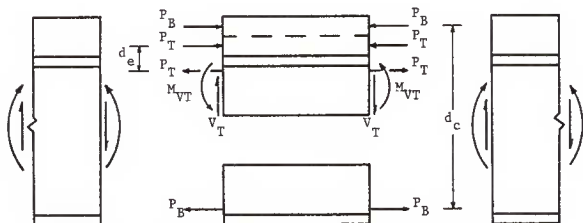


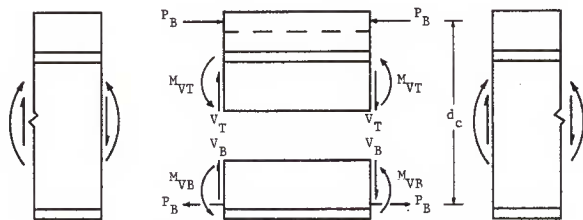
Fig. 3 Four Hinge Failure Mechanism



a. Case I Pure Bending ( $V = 0$ ,  $M = P_B d_c + M_e$ ,  $M_e = P_T d_e$ )

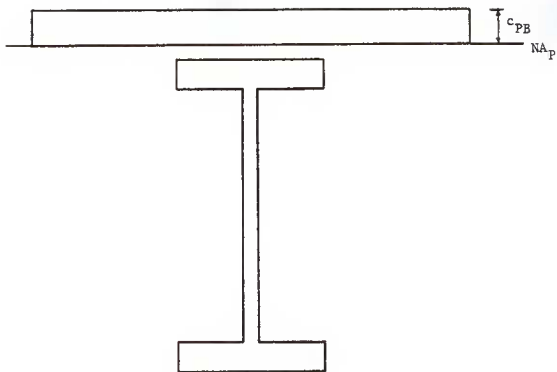
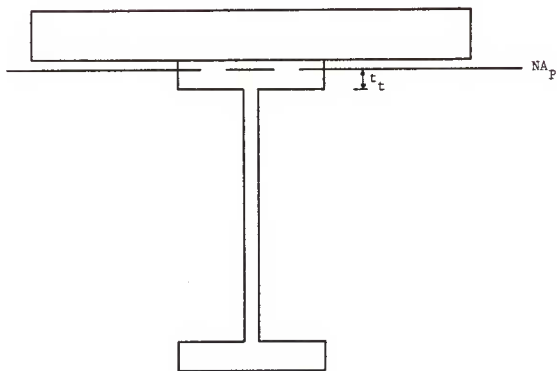


b. Case I General ( $M_{VT} = V_T a$ ,  $M = P_B d_c + M_e$ ,  $M_e = P_T d_e$ )



c. Case II General ( $V = V_T + V_B$ ,  $M_{VT} = V_T a$ ,  $M_{VB} = V_B a$ ,  $M = P_B d_c$ )

Fig. 4 Internal Forces at Opening

a.  $NA_p$  in Slabb.  $NA_p$  in FlangeFig. 5 Sections for  $M_{Pc}$



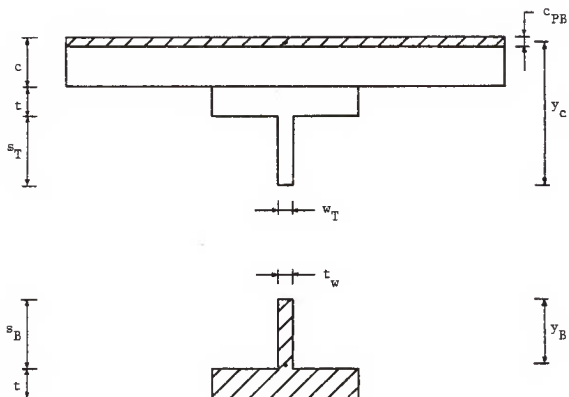


Fig. 6 Axial Force in Bottom Tee - Case I

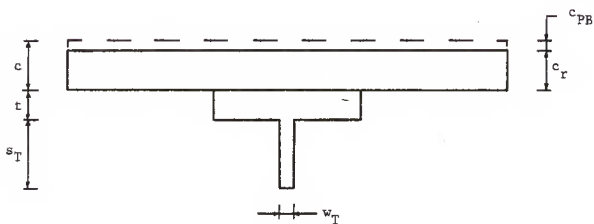


Fig. 7 Top Tee - Remaining Concrete Section

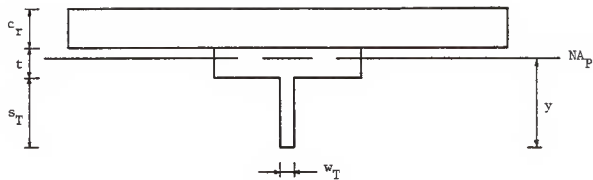
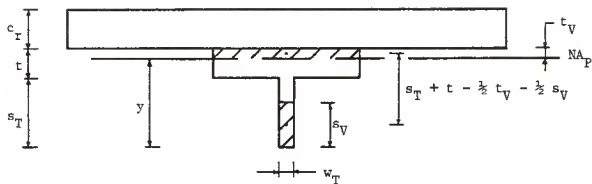
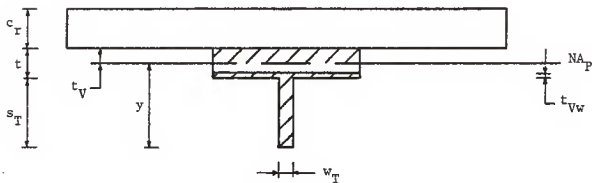


Fig. 8 Case IA -  $NA_p$  in Flange

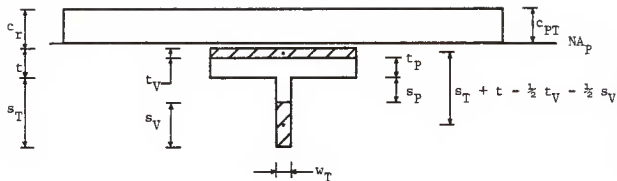


$$a. \quad s_V < s_T$$

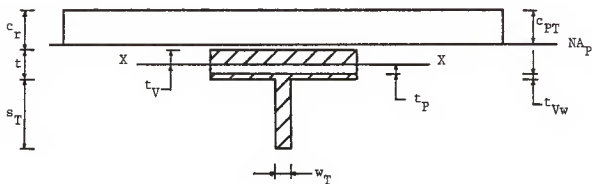


$$b. \quad s_V > s_T$$

Fig. 9 Case IA



a.  $s_V < s_T$



b.  $s_V > s_T$

Fig. 10 Case IB

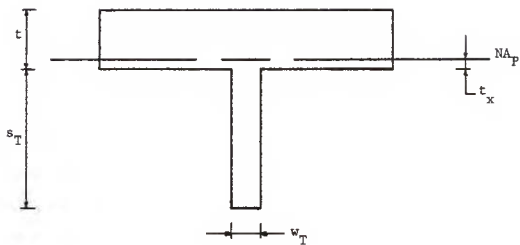


Fig. 11 Top Tee Case II

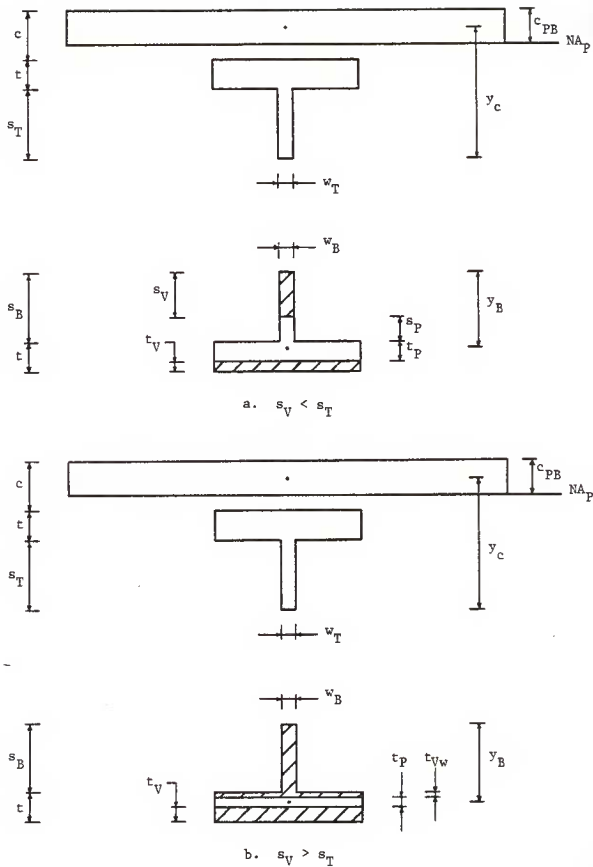


Fig. 12 Case II

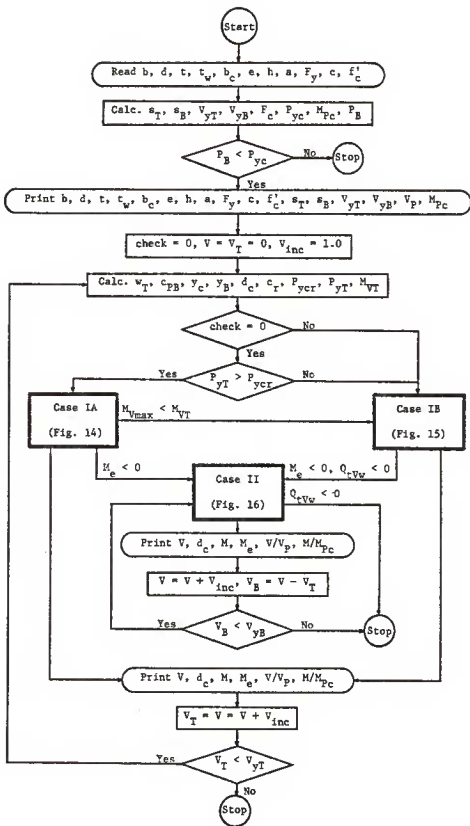


Fig. 13 General Flow Diagram

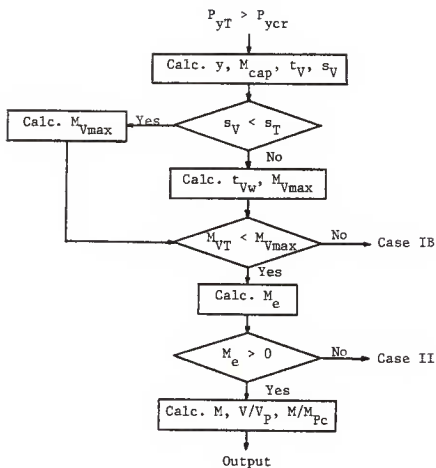


Fig. 14 Flow Diagram for Case IA



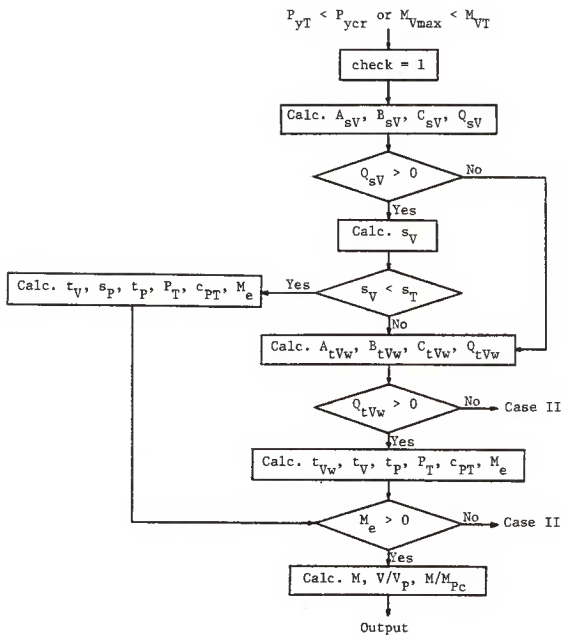


Fig. 15 Flow Diagram for Case IB

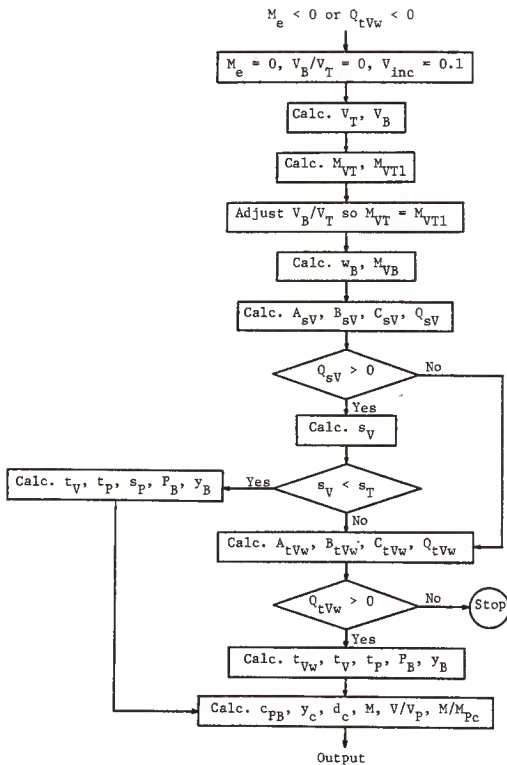


Fig. 16 Flow Diagram for Case II

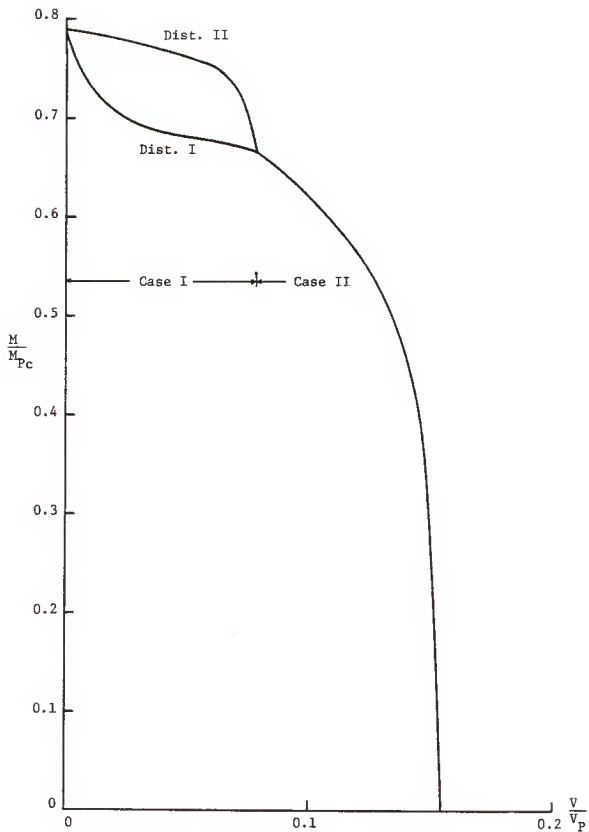
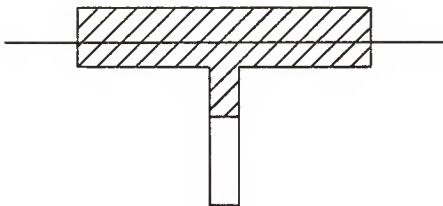
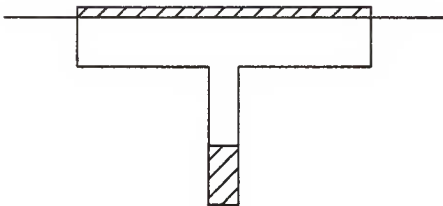


Fig. 17 Interaction Diagram

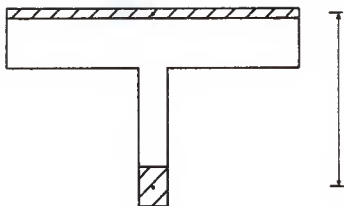


a. Distribution I

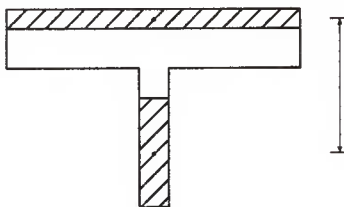


b. Distribution II

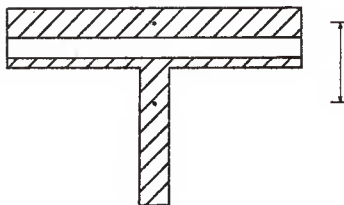
Fig. 18 Methods of Shear Moment Distribution



a. Low Shear



b. Increased Shear



c. High Shear

Fig. 19 Changes in Moment Arm for  $M_{VT}$

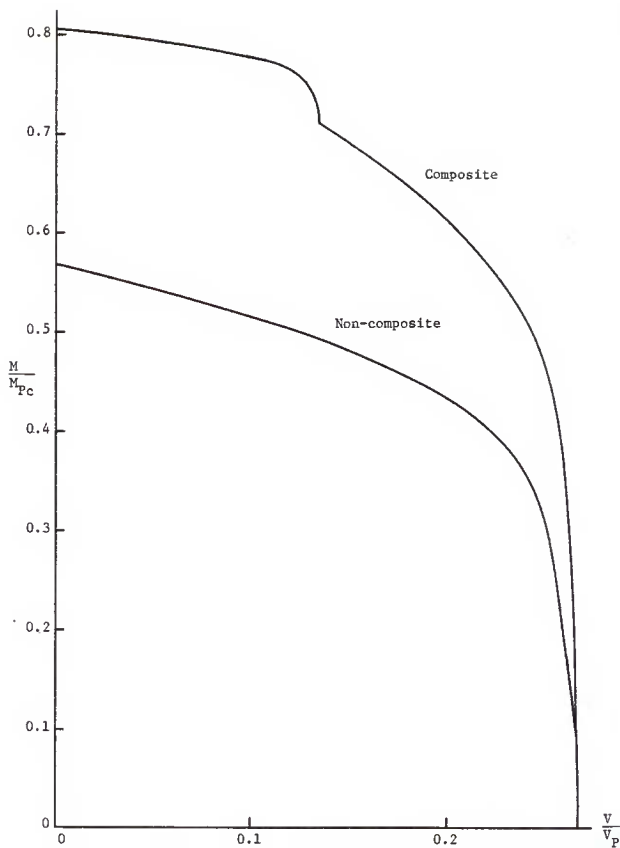


Fig. 20 Interaction Diagrams for Composite and Non-composite Beams

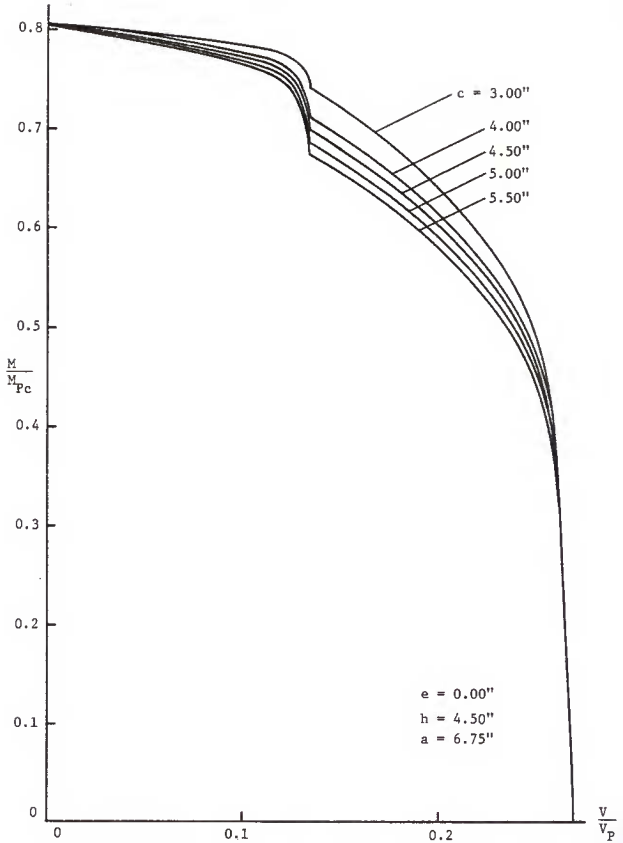


Fig. 21 Effect of Varying Slab Thickness

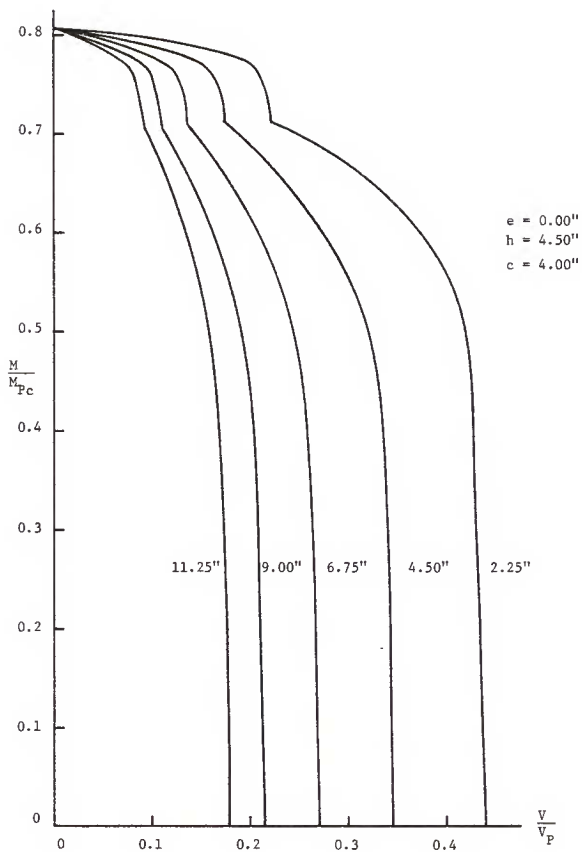


Fig. 22 Effect of Varying Opening Length



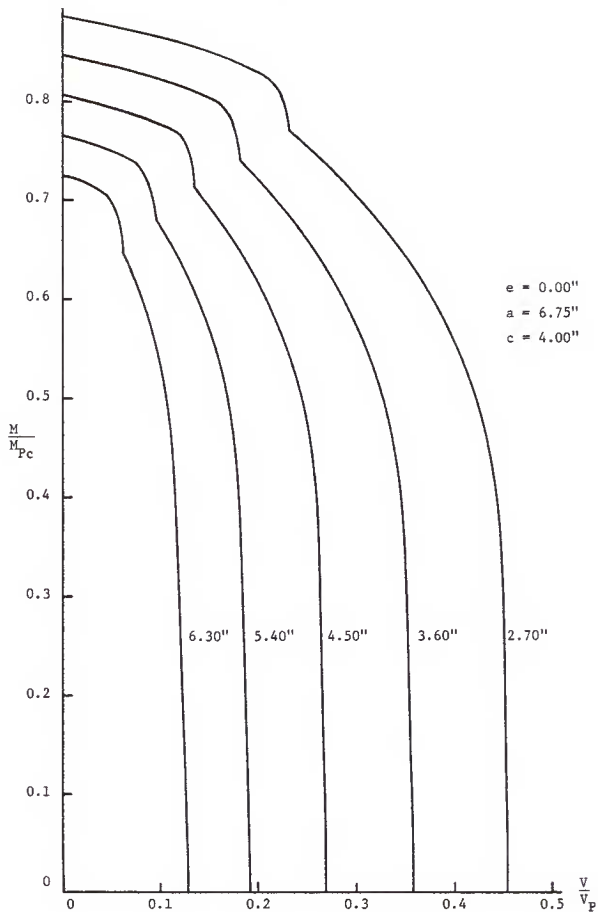


Fig. 23 Effect of Varying Opening Height

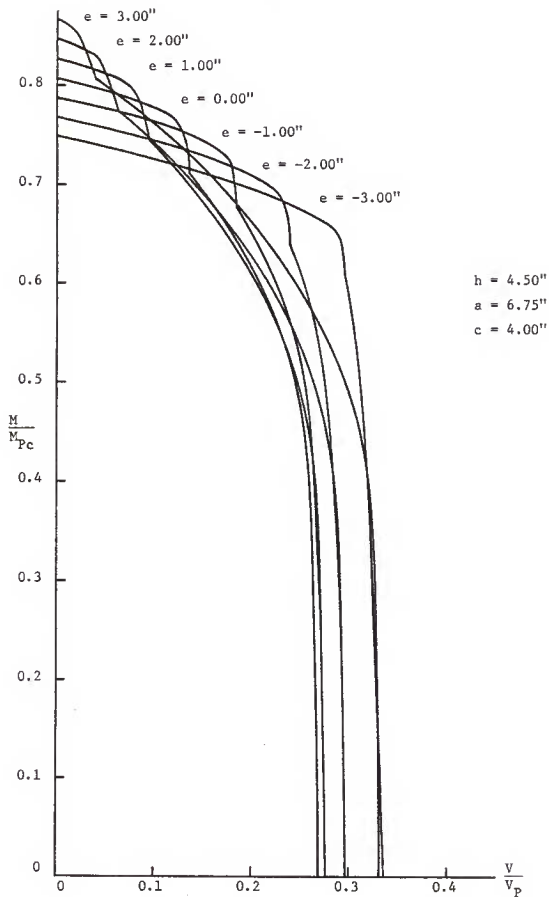


Fig. 24 Effect of Varying Eccentricity

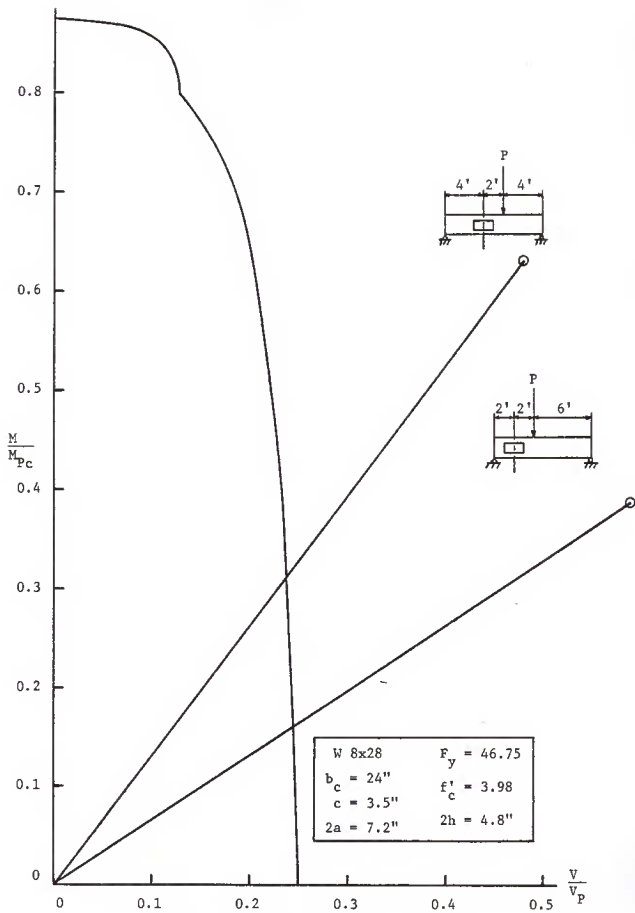


Fig. 25 Test Results from Reference 5

STRENGTH OF COMPOSITE BEAMS WITH WEB OPENINGS

by

DAVID MARTIN TODD

B. S., Kansas State University, 1977

---

AN ABSTRACT OF A MASTER'S THESIS

Submitted in partial fulfillment of the  
requirements for the degree

MASTER OF SCIENCE

Department of Civil Engineering

KANSAS STATE UNIVERSITY  
Manhattan, Kansas

1979

## ABSTRACT

The purpose of this thesis is to present an ultimate strength analysis of composite beams with web openings. With the use of this analysis certain variables were studied and the following conclusions were drawn:

1. Changes in the slab thickness do not affect the interaction diagram to a large extent.
2. The longer the opening is, the smaller the failure load,
3. As the opening is made deeper, the moment and shear capacity decrease.
4. An opening with the highest positive eccentricity has the highest moment capacity.

Theoretical results based on the analysis provide a very conservative prediction of the strength of test beams. This is thought to be primarily due to the assumption that the concrete slab does not carry any shear force.